## Chapter 1

# Introduction to Scanning Probe Microscopy

Today's research laboratory is required to solve difficult problems that span multiple disciplines. Advanced techniques are required to answer pressing questions related to adhesion, bonding, contamination and surface cleanliness, corrosion, surface morphology, surface roughness, surface topography, failure analysis, process monitoring, surface chemistry, biological characterization, local surface properties — both electrical and mechanical, and thin film analysis. Rarely can one analytical technique effectively span such a wide range of applications. The rapid rise of scanning probe microscopy (SPM) provides a truly marvelous tool that provides useful information about all these topics and many more.

Few scientific instruments have received as much attention and enjoyed such rapid growth as the atomic force microscope (AFM). The inherent simplicity of the AFM coupled with its ability to apply nanoNewton forces to surfaces with sub-nanometer lateral precision have led to a significant expansion in both the scope and context of the instrument. Originally used to probe the atomic roughness of a surface, the AFM has quickly evolved into a probe of surface forces using primarily only two modes of operation (contact and dynamic). Of particular significance are the rapidly evolving techniques that allow quantitative material property maps of surfaces with nanometer-scale resolution. Furthermore, the ability to position and precisely move a biased tip has been exploited to demonstrate novel nanoscale device fabrication. Taken together, these developments have led to the widespread use of AFM in all fields of science and engineering.

The intelligent use of SPM and AFM requires broad training in a multitude of different disciplines spanning many areas of science and engineering.

New graduate students, when asked to use an AFM ask many questions: How do I choose a cantilever? How fast should I scan? How do I optimize the feedback? What should I do to reduce noise? How can I improve resolution? What's the best way to prepare a sample? After many years of answering such "how to?", "what should I do?" questions one at a time, I found it more useful to first teach my students at Purdue the fundamentals of how an AFM works. These lecture notes are the logical consequence of this approach. In writing this book, I have two main goals: (i) to convey to a beginning student the scope of knowledge required to properly use an AFM, and (ii) to convey a clear understanding of the physics and mathematical models underlying AFM. If these two goals are met, then students should have the necessary tools to provide answers to many important and vexing questions as they arise. There are numerous seminars, power point presentations and monographs available on the web that survey different imaging modes and provide helpful hints to technical questions about image optimization and sample preparation. What is lacking is an extended discussion about the physics and mathematics underlying the AFM coupled with a discussion about the fundamentals of AFM design, its operation and its use. We find very little in the way of a systematic discussion of the fundamentals of AFM, a topic that forms the focus of these lecture notes.

## 1.1 Historical Perspective

The generic SPM is an extremely versatile instrument that has steadily evolved from its invention in the early 1980s. In these lecture notes, SPM is used to broadly denote the two most popular scanning probe instruments, the scanning tunnelling microscope (STM) and the atomic force microscope (AFM). SPMs are now routinely available in many research labs throughout the world and are widely heralded for ushering in the study of matter at the nanoscale.

The underlying principles of an SPM are quite simple but yet completely different in many significant ways from more traditional microscopes. Essentially, the SPM works by positioning a sharp tip (often called a proximal probe) about 1 nanometer above a substrate. The highly local information provided by the microscope is achieved by a combination of the sharpness of the tip as well as the small separation between the tip and substrate. The critical feature of any SPM is the ability to maintain a

constant tip–substrate distance (with a precision approaching a few picometers) while the tip is rastered across the substrate in a highly controlled way. While it is important that the tip–substrate distance be held constant, it is surprisingly difficult to accurately know the exact value of this distance.

To achieve high precision, a signal must be acquired that is very sensitive to the tip–substrate separation. The exact physical origin of this signal then determines the property of the substrate that is mapped. A key discovery during the development of SPMs was the realization that with a sufficiently sharp tip, a quantitative 3-dimensional image of surfaces can be obtained, often with atomic resolution.

The worldwide interest in scanning probe instruments was ignited by the research accomplishments of G. Binnig and H. Rohrer at the IBM Zurich Research labs in Switzerland [binnig87]. These two individuals shared the 1986 Noble Prize in Physics (along with E. Ruska, inventor of the electron microscope) for their seminal work in the invention of SPM [binnig82], [binnig83a], [binnig83b], [binnig86]. A reading of the published literature has revealed relevant prior art that resemble the implementation of the first SPM in the early 1980s. Work on surface profilers (using optical deflection techniques similar to those used in current scanning force microscopes) can be found in the published work of G. Shmalz that dates to 1929 [shmalz29]. R. Young, J. Ward and F. Scire developed in 1972 an instrument (called a topografiner) designed to measure the surface microtopography of a substrate [young71], [young72]. This work utilized a controllable metal-vacuum-metal separation to maintain a fixed tip–substrate distance, in some sense foreshadowing by some 10 years the tunnel gap approach developed independently by Binnig and Rohrer.

Before beginning an in-depth study of an AFM, it is useful to first discuss the general principles underlying *all* SPMs. The two widely-used families of SPMs — the STM for studying the surface topography of *electronically conducting* substrates and the AFM, developed to investigate the surface topography of *electrically insulating* substrates. The proliferation and development of SPM technology has greatly benefitted from parallel developments in both fields of STM and AFM, generating a wide variety of dual probe implementations of hybrid SPMs (sometimes called SxMs; where x stands for some physical variable of interest), which have led to simultaneous measurements with high lateral and vertical resolution not only of surface topography but also of other local properties of substrates.

## 1.2 The Need for a Scanning Probe Microscope

When invented, the STM was a unique instrument because it relied on proximal probe techniques to interrogate very local properties of an electrically conducting sample. The data obtained were able to resolve individual atoms by providing a 3-dimensional image, a seemingly commonplace occurrence today but quite a remarkable achievement in the 1980s.

The ability to view an inanimate object in 3-dimensions dates back to the 1840s when the stereo pair concept was invented, and has been used extensively for military and geographical (terrain) applications, and in more modern times for entertainment purposes. A map of individual atom positions was first achieved using the field-ion microscope [muller56] and had developed into an active field of research by the mid-1960s [muller65]. But the ability to couple these two capabilities into a single widely accessible instrument was a truly remarkable development that enabled world-wide experiments in many scientific disciplines.

Traditional electron microscopy (e.g., transmission electron microscopes (TEM) and scanning electron microscopes (SEM)) rely on the small size of the de Broglie wavelength of electrons to provide sufficient resolution to view sub-micron features on conducting surfaces. The use of these microscopes has grown continuously since their resolution surpassed optical microscopes shortly after their invention in the early 1930s. By the 1960s, TEMs were capable of 0.3 nm resolution while SEMs were able to resolve objects in the 15–20 nm range. By the 1980s, wide-spread improvements in instrumentation enabled analytical applications of electron microscopes that included energy dispersive x-ray spectra, electron energy loss spectroscopy, and the development of high resolution imaging theory [haguenau03].

In spite of these successes, the ability to combine compositional identification with electrical and/or mechanical measurements at select locations on a sample surface was a noticeable limitation of the many new surface science tools that were rapidly developed in the 1970s. This clearly identified need, evident in both academic and industrial research labs around the world, might explain the rapid acceptance of SPMs once their basic capabilities were demonstrated. While freely admitting that the attributes and shortcomings of each technique are a matter of personal taste, Table 1.1 attempts to compare TEM, SEM, and SPM.

Finally, it should be remarked that any student working in the world of sub-micron science or engineering requires a good knowledge of many

Table 1.1 A brief summary of the attributes of different sub-micron microscopies in common use in a modern research laboratory.

| | TEM | SEM | SPM |
|---|---|---|---|
| *Notable Attribute* | Atomic Resolution | Depth of Field | High contrast in z plus high lateral resolution |
| *Major Limitations* | Extensive sample preparation of thin specimens; sample modification under e-beam irradiation; initial expense is high | Requires electrically conducting samples, extensive training often required, high cost of equipment maintenance | Speed of image acquisition, special training often useful |
| *Dimensions Probed* | 2-D, planar | 2-D, planar | 3-D |
| *Notable Capability* | Atomic resolution | Chemical Composition | Topography plus Physical Properties |
| *Environment* | High Vacuum | Primarily Vacuum | Vacuum, Air, Liquid |

characterization tools to produce credible research results. Knowing which tool to use in what situation can save considerable time in the pursuit of definitive answers to pressing problems. The choice of techniques are large and must include light microscopy, TEM, SEM, SPM, X-ray diffraction (XRD), X-ray Photoemission Spectroscopy (XPS) for elemental analysis, electron spectroscopy (UV photoemission, LEED) for surface analysis, and vibrational spectroscopy (HREELS, FTIR and Raman scattering) for molecular analysis.

## 1.3 The Scanning Tunneling Microscope

The STM was historically the first SPM and was introduced in 1982 by G. Binnig and H. Rohrer with the demonstration that a controllable vacuum tunnelling gap could be achieved between a sharp metallic tip and a conducting substrate [binnig82]. The vertical resolution of the STM is a few picometers while the lateral resolution can range down to $\sim$0.1 nm on an atomically flat substrate. STM images typically span an area ranging from a few nanometers to a few 100's of nanometers.

To understand tunnelling through a vacuum gap, knowledge of quantum mechanics, solutions to Schrödinger's wave equation and a basic understanding of electron states in metals are required [gomez05]. Since STM is

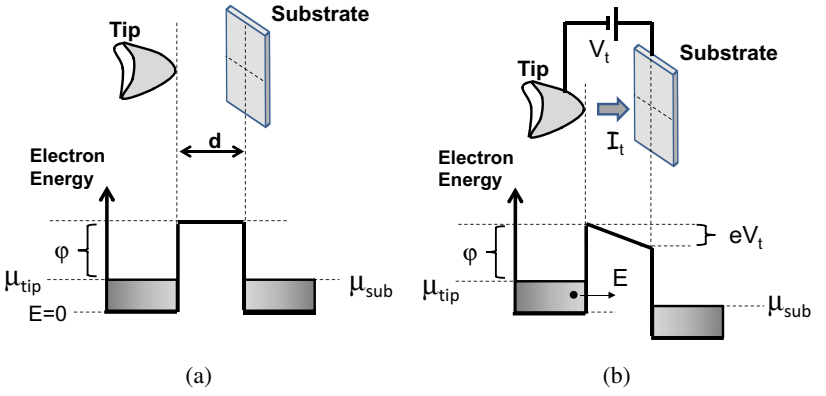


Fig. 1.1 In (a), a schematic of the potential barrier of width d (∼1 nm) between a metallic tip and metallic substrate. In equilibrium, the electrochemical potential of the tip ($\mu_{\text{tip}}$) and that of the substrate ($\mu_s$) are aligned. The height of the potential barrier is $V_o = \varphi + \mu_{\text{tip}}$. In (b), the situation that develops when a bias voltage ($V_t$) is applied between tip and substrate. A tunnel current ($I_t$) comprised of electrons with various energies E can arise even though there is no physical contact between the tip and substrate.

not the main focus of this book, we refer those not familiar with these topics to textbooks that discuss tunneling in a straightforward way [tipler12]. Electron tunnelling is usually discussed for the ideal case when an electron with incident energy $E$ encounters a barrier with a characteristic width $d$ and a characteristic height $V_o$. The situation is shown in Fig. 1.1(a).

Such a barrier develops in the physical gap between a tip and substrate with a height $V_o = \varphi + \mu_t$ where $\varphi$ (typically 4–5 eV; $1\,\text{eV} = 1.602 \times 10^{-19}$) represents the work function of the metal tip and $\mu_{\text{tip}}$ (typically 5–10 eV) represents the value of the Fermi energy, the most energetic electron in the tip. The presence of this barrier prevents the transit of a classical electron, but within the context of quantum mechanics, the electron is treated as a wave and it has a finite probability of penetrating the barrier.

The underlying physics required to understand how an STM operates begins by considering electrons incident upon a barrier at an energy $E < V_o$. Such electrons can quantum mechanically tunnel through the barrier with a transmission probability $T$ that can be obtained from a time-independent solution to Schrödinger's Equation. For a rectangular barrier, the transmission probability is given by [tipler12]

$$T = \frac{4E(V_o - E)}{4E(V_o - E) + V_o^2 \sinh^2(\kappa d)} \quad E < V_o. \tag{1.1}$$

The wavevector of the electron when tunnelling is defined by

$$\kappa \equiv \frac{2\pi}{h}\sqrt{2m(V_o - E)}, \tag{1.2}$$

where $m$ is the electron mass ($9.109 \times 10^{-31}$ kg) and $h$ is Planck's constant ($6.626 \times 10^{-34}$ Js). When $\kappa d \gg 1$ (an approximation appropriate for STM experiments), Eq. (1.1) reduces to the well-known result that

$$T \simeq \frac{16E(V_o - E)}{V_o^2} e^{-2\kappa d}. \tag{1.3}$$

If $E \cong \mu_{\text{tip}}$ as is the case for low applied bias, then $V_o - E \cong \varphi$, the work function of the metal surface. Since $\varphi$ is about 5 eV, the coefficient $2\kappa$ appearing in Eq. (1.3) is approximately $23\,\text{nm}^{-1}$.

For an electrical current $I_t$ between the tip and substrate, a bias voltage $V_t$ must be applied as shown in Fig. 1.1(b). This bias voltage will distort the shape of the square barrier, which will also be rounded and lowered in height by many-body electron correlation effects not considered here. The electric current between tip and substrate will be approximately proportional to the transmission probability defined in Eq. (1.3) for a square barrier. Since the measured current will be comprised of tunnelling electrons with different energies $E$, after integration over an appropriate range of energies, the tunnel current $I_t$ will be given by an expression of the general form

$$I_t \simeq f(V_t, \varphi) e^{-2\kappa d}, \tag{1.4}$$

where $f(V_t, \varphi)$ is a function that depends on the applied voltage and the exact shape of the barrier under consideration. The exact barrier shape is difficult to determine, which explains why the analytical result for a square barrier is so often invoked. For applied voltage differences of $\sim$1 V, typical tunnel currents encountered in STM experiments lie between 0.01 nA and 1 nA, depending on the value of $d$.

The strong exponential dependence of $I_t$ with distance $d$ is the important point to remember from this discussion. Rough estimates using Eq. (1.3) indicate that a change in the barrier width $d$ by 0.1 nm causes a change in $I_t$ by roughly a factor of 10. This large amplification implies that small tip motions can be easily detected, measured and hence controlled. This key realization opens the door to a practical STM.

The exquisite sensitivity of $I_t$ to tip–substrate separation $d$ is used to monitor the vertical tip position above a substrate and hence transform tunnel current variations into high magnification images of a sample. Two modes of imaging have been developed: (a) constant height imaging in which

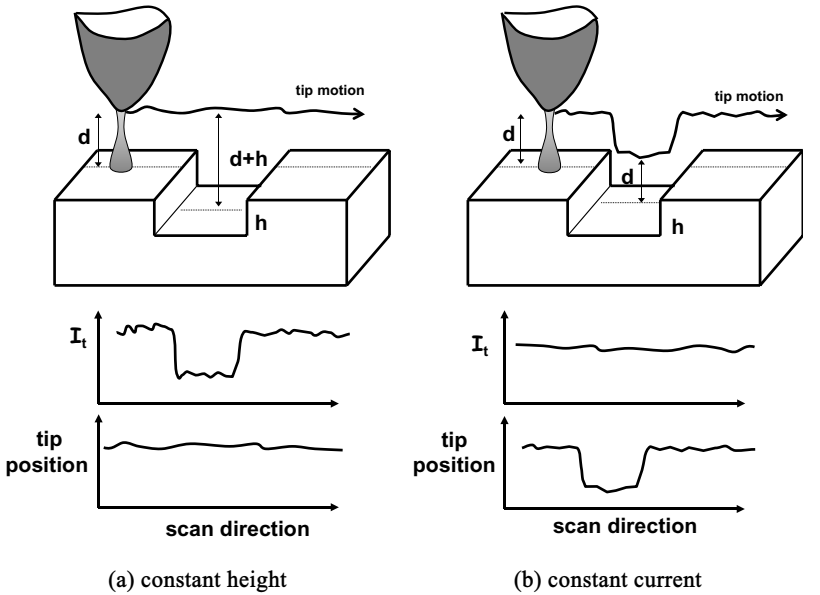


Fig. 1.2 A schematic illustrating two modes of imaging employed in STMs. In (a), the tip–substrate separation is fixed and the variations in tunnel current $I_t$ are related to variations in $d$. In (b), the tunnel current $I_t$ is held constant by a feedback loop and the relative tip-substrate separation is varied to maintain a constant tunnel current.

the tip is moved at a fixed height above the substrate while variations in tunnel current due to height variations are recorded and (b) constant current imaging in which the tip position is continually adjusted by a feedback loop to produce a constant tunnel current. These two modes of imaging in STM are illustrated in Fig. 1.2.

The constant height mode illustrated in Fig. 1.2(a) is of limited use unless the sample surface is atomically flat since the tip position is not dynamically adjusted. In this mode of operation, the current variation is recorded as the tip is scanned across the substrate. This mode is most appropriate for substrates that are flat at the atomic length scale. Furthermore, since variations in tunnel current measured in the constant height mode depend exponentially with distance, observed variations in $I_t$ cannot be directly interpreted as height profiles. The 3-dimensional imaging capability of STM is most easily understood by considering the constant current imaging mode shown in Fig. 1.2(b). An STM image results when the relative motion of the substrate is recorded while maintaining a constant

tunnel current $I_t$ as the tip is swept across a pre-selected area of the substrate. To achieve this, a high-gain current amplifier (typical gain is $\sim 10^8$ to $\sim 10^9$ V/A) is required.

Sharp tips are necessary to produce images with high lateral resolution. Common ways of producing STM tips from metal wires (such as W or Pt) with diameters of $\sim 1 \times 10^{-4}$ m rely on electrochemical etching or physical cutting, followed by thermal annealing and sharpening in ultra-high vacuum. The reliable formation of sharp tips may seem like a daunting venture, but ultimately every tip formed must end with one (or possibly a few) atoms which ever so slightly protrude from the apex, forming a small mini-tip at the tip's apex. The presence of such mini-tips, along with the strong exponential drop-off of current with distance, provides a sensible way to understand why the total tunnel current between tip and substrate is dominated by an atomically small protrusion from an otherwise large tip.

Complete theories of STM have shown that the tunnel current can be related to the quantum wavefunction overlap between electron states in the tip and electron states in the substrate. This implies that the images obtained from an STM contain not only surface topographic information, but also information about the variation of the local density of electronic states. This complication provides a caveat against the interpretation of relative tip–substrate separation into surface topographic features. STM images are notable for the amazing detail they reveal about the atomic periodicity and surface morphology of clean, electronically conducting substrates.

## 1.4 The Atomic Force Microscope

While STMs provide a quantitative map of surface topography with atomic resolution, they suffer from a fundamental limitation that the substrate studied must be sufficiently conducting to support a tunnel current, a limitation that was recognized early in the development of the STM. In order to overcome this difficulty, an AFM was first demonstrated in 1986 by Binnig, Quate and Gerber [binnig86]. The operation of an AFM relies on the surface forces acting on a sharp tip in close proximity to a surface, a topic that will be discussed in detail in the coming chapters. These surface forces are ubiquitous and exist between tips of any material and substrates of any material. From the very beginning, AFM promised to solve the problem of atomically-resolved images of insulting substrates.

For sufficiently small tip–substrate separations, these interaction forces can range from 10's of pN to 10's of $\mu$N, with typical values of a few tens of nN. An understanding of these interaction forces is central to understanding how an AFM functions. Most importantly, these forces are not predicated on the fact that either the tip or substrate be electrically conducting. Because of the long-range nature of the interaction forces, the vertical resolution of an AFM is typically less than a nanometer (comparable to an STM) while the lateral resolution is determined by the tip radius and sample roughness and is generally somewhat larger than that for STMs. In contrast to STM, which focusses on ultra-clean surfaces that are atomically flat, AFMs are used to study a wide variety of different substrates — both rough and smooth. AFM images typically span an area ranging from a ~100 nm to ~10's of $\mu$m.

In practice, the operation of an AFM relies on a sharp tip that is usually supported on the end of a microcantilever whose minute deflections can be carefully monitored. As shown in Fig. 1.3, when a microcantilever with spring constant $k_c$ (units of N/m) positions a tip distance $z$ from a substrate, the cantilever will deflect toward the substrate by an amount $q$ due to attractive interaction forces that exist between the tip and substrate.

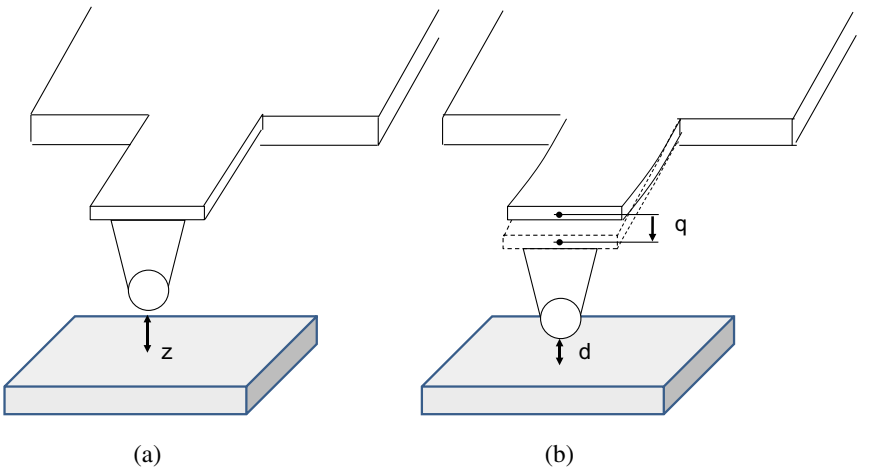


Fig. 1.3 A schematic illustrating the sequence of events when a tip on a microcantilever is brought into close proximity to a substrate. In (a), the apex of the tip is located a distance $z$ above the substrate. Attractive surface interaction forces between the tip and substrate bend the tip toward the substrate until a deflection $q$ of the cantilever brings the system into equilibrium. The final tip-substrate separation is indicated by the parameter $d$.

Table 1.2 A few representative AFM cantilevers commercially available with their characteristic dimensions, spring constants, and resonant frequencies.

| material | length | width | thickness | $k_c$ (N/m) (min, typical, max) | $f_o$ (kHz) (min, typical, max) |
|---|---|---|---|---|---|
| Si | $125 \pm 5\,\mu$m | $35 \pm 3\,\mu$m | $4.0 \pm 0.5\,\mu$m | 20, 40, 75 | 265, 325, 400 |
| Si | $230 \pm 5\,\mu$m | $40 \pm 3\,\mu$m | $7.0 \pm 0.5\,\mu$m | 25, 40, 60 | 150, 170, 190 |
| Si | $90 \pm 5\,\mu$m | $35 \pm 3\,\mu$m | $2.0 \pm 0.3\,\mu$m | 6.5, 14, 28 | 240, 315, 405 |
| Si | $125 \pm 5\,\mu$m | $35 \pm 3\,\mu$m | $2.0 \pm 0.5\,\mu$m | 1.8, 5.0, 12.5 | 110, 160, 220 |
| Si | $90 \pm 5\,\mu$m | $35 \pm 3\,\mu$m | $1.0 \pm 0.3\,\mu$m | 0.45, 1.75, 5.0 | 95, 155, 230 |
| Si | $300 \pm 5\,\mu$m | $35 \pm 3\,\mu$m | $1.0 \pm 0.3\,\mu$m | 0.01, 0.05, 0.1 | 9.5, 14, 19 |

For sufficiently small deflections, the cantilever motion can be well approximated in terms of Hook's law, which predicts an upward restoring force proportional to the cantilever deflection $q$ given by

$$F_{restoring} = -k_c q. \tag{1.5}$$

In equilibrium, this restoring force must be equal and opposite to the interaction force that caused the deflection.

Table 1.2 provides typical dimensions and relevant properties of a few microcantilevers that are commercially available for use in AFM applications. Any uncertainty in cantilever thickness can cause considerable uncertainty in the resulting spring constants. Sharp tips, with effective radius $R$ (typically $R$ is between 5 and 30 nm), are routinely fabricated onto these cantilevers using lithographic techniques in common use by the microelectronic semiconductor industry. The wide-spread availability of suitable microcantilevers has enabled the routine measurement of interaction forces of order 1 nN between tip and substrate. Typically this means that cantilever deflections of order 1 nm or less can be detected.

To measure cantilever motion while scanning, a high-gain transducer of cantilever deflection plus a feedback mechanism is required. A variety of techniques — capacitance, optical interferometery, piezoelectric microcantilevers, and optical beam deflection — have been successfully implemented to accurately detect cantilever deflection. Each technique seems to have its own advantages. At this point in time, the technique most often implemented is an optical deflection scheme shown schematically in Fig. 1.4.

Using this approach, a laser is focused on the cantilever and the reflected light is directed onto a segmented photodiode. Fine positioning of the

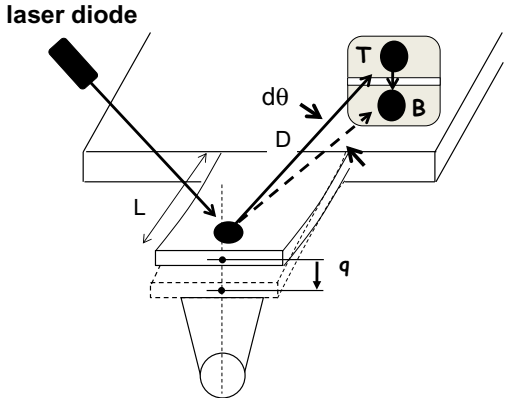


Fig. 1.4 A common method employed to measure the deflection of a cantilever is a beam bounce technique in which a diode laser beam is reflected from a microcantilever onto a segmented photodiode. By monitoring the voltage produced by the top (T) and bottom (B) segment of the photodiode, the relative motion of the reflected laser spot can be monitored and information about sub-nanometer deflection $q$ of the cantilever can be inferred.

reflected spot on the photodiode allows for a null condition to be achieved. This occurs when the voltage from the top photodiode segment (T) equals the voltage from the bottom photodiode segment (B) in Fig. 1.4. A small cantilever deflection disrupts this null condition, giving rise to a voltage proportional to deflection. The origin of the high amplification for this particular system follows from simple geometrical considerations. For a cantilever displacement $q$, the reflected laser spot moves a distance $\Delta s$ which is approximately given by

$$\Delta s \simeq q\frac{D}{L}, \tag{1.6}$$

where $D$ is the distance of the cantilever from the photodiode and $L$ is the cantilever's length. Typically, the ratio of $D/L$ for an AFM microcantilever can easily be a factor of 100–500.

When discussing the nature of the interaction force between tip and substrate, it is often convenient to approximate the tip as a sphere with radius $R$ as shown in Fig. 1.4. This sphere then interacts with the substrate via a number of possible forces that cause the cantilever to deflect.

The exact details of the relevant interaction forces, as well as their variations on $d$, depend to a large extent on the composition of the tip and substrate and will be further discussed in Chapters 2–4. For the ideal case

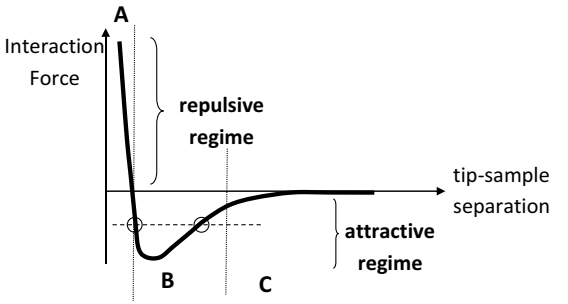


Fig. 1.5 A schematic illustrating how the interaction force between tip and substrate varies as a function of separation. Three regions (A, B, C) are indicated. Different modes of imaging are achieved when the tip is positioned in each region.

of a clean and electrically neutral tip positioned above a clean and electrically neutral substrate in ultra-high vacuum, the interaction forces might be well-approximated by a superposition of a short-range, hard-wall repulsion (effective when the tip–substrate separation is less than $\sim$0.3 nm) plus a longer range surface interaction due to the van der Waals (vdW) force acting between dipoles induced on the individual atoms comprising the tip and substrate. The variation of this interaction force on tip–sample separation is related to the detailed shape of the substrate and tip. If the system is operated under ambient air conditions, hydration forces due to adsorbed water or long-range electrostatic forces due to uncontrollable charging of the tip or substrate may well dominate.

Without a detailed knowledge of the system under study, it is difficult *a priori* to accurately specify a force vs. distance relationship. In general, such an interaction might be expected to follow the approximate shape shown in Fig. 1.5. This figure qualitatively illustrates (i) the attractive regime ($F < 0$) in which the interaction forces cause the microcantilever to bend toward the substrate and (ii) the repulsive regime ($F > 0$) that causes the microcantilever to bend away from the substrate when the tip comes into contact with it.

If the tip is in region A in Fig. 1.5, then imaging is performed in *contact mode*; the tip exerts a force directly on the sample as it is scanned across it. In contact mode imaging, the direct up and down motion of the cantilever is measured while scanning. A 3-dimensional image is built up as the sample is rastered beneath the tip. Usually, a feedback circuit raises and lowers the sample in such a way that the cantilever deflection remains constant. The amount the sample is raised or lowered at each $(x, y)$ position forms the

"topographical" image of the sample's surface. This motion can be used to produce a 3-dimensional image of the substrate in much the same way as a conventional profilometer, except now the applied force lies in the nN range and the radius of the stylus is in the 5–30 nm range.

This mode of operation can be damaging, especially for soft substrates and stiff microcantilevers since significant lateral forces develop during the scanning process. The contact regime of operation plus the underlying topics required to understand AFM in general are discussed in this volume of the lecture notes.

If the tip is in Region C of Fig. 1.5, the interaction forces are sufficiently weak so that very small deflections of the cantilever result. Since the substrate–tip separation is relatively large, imaging in this region is often referred to as the *non-contact mode*. Under these circumstances, indirect detection schemes are usually employed. As an example in non-contact mode imaging, the tip is often driven sinusoidally at a frequency near its mechanical resonance. Small position-dependent shifts in the resonance frequency then occur as the substrate is rastered beneath the tip. These frequency shifts provide a sensitive measure of tip–substrate interaction, thereby providing an input signal for a suitable feedback controller that adjusts the substrate position to maintain a constant frequency. The adjustments in the substrate position are then interpreted as a 3-dimensional topographic map of the surface structure. Because of the low forces applied to the sample, this mode is often preferred when studying soft substrates.

If the tip lies in Region B of Fig. 1.5, the slope of the interaction force becomes comparable to the restoring force of the microcantilever, implying that static tip displacements, although measurable, may not be reliable because of resulting instabilities. The instabilities arise because of the double-valued nature of the interaction force as illustrated schematically by the horizontal dotted line in Fig. 1.5, which shows that for the same value of the interaction force, there are two possible tip–sample separations. These instabilities are often referred to as jump-to-contact because the tip spontaneously snaps into contact with the substrate no matter how careful an approach procedure is followed. To scan in region B, the tip must be driven in a sinusoidal motion that is accurately monitored by the AFM control electronics. During the tip's motion, the tip will periodically come into contact with the substrate (Region A in Fig. 1.5), giving rise to what is known as *intermittent-contact* or *tapping mode* imaging. A careful

analysis of the tip motion in this regime relies on solving the appropriate non-linear differential equations, a topic that will be covered in the 2nd volume of the lecture notes *Fundamentals of Atomic Force Microscopy, Part II: Dynamic AFM*. The added complication due to a non-linear tip motion has the advantage that property maps of sample stiffness, adhesion, etc. can be correlated with 3-dimensional topographic images.

The boundaries between the different regions in Fig. 1.5 are not necessarily well-defined. There is considerable discussion of these different regimes in the literature, so a precise distinction between them is challenging. For our purposes, this discussion might best be left to the opinion of experts. Suffice it to say, when the tip is oscillating, all Regions A, B and C are probed, and the AFM is often then referred to as a Dynamic Force Microscope (DFM). The imaging process is often referred to as dynamic mode imaging.

It is worth mentioning that a less complicated way of implementing intermittent contact mode imaging is to use an alternative approach often referred to as *jumping mode*. In this procedure, the cantilever does not undergo sinusoidal motion but instead follows a motion determined by software controlling the AFM. In practice, the software is programmed to position the tip at a distance far from the substrate, and then drive the substrate toward the tip under feedback control until the cantilever bending reaches a preset loading force. At this point the z-displacement of the substrate required to meet this preset loading condition is measured and the tip is withdrawn, moved to a nearby adjacent location above the substrate where the process is again repeated.

Upon completion of each 'jump', various features of the cantilever displacement as a function of the z-motion of the substrate are extracted from the data and plotted for further analysis. The advantage of this technique is that the force acting on the tip can be carefully monitored during the process by recording what is commonly called force vs. distance data. Furthermore, the lateral force imparted to the substrate while scanning is eliminated. The disadvantage is that a 'jump' image proceeds at a somewhat slower rate than when the cantilever is sinusoidally driven.

Figure 1.6 provides a schematic summary diagram of these different imaging modes.

Each of these modes of imaging requires different measurement techniques and control electronics. In addition, the mechanical properties of the cantilever must be selected for each technique to optimize success.

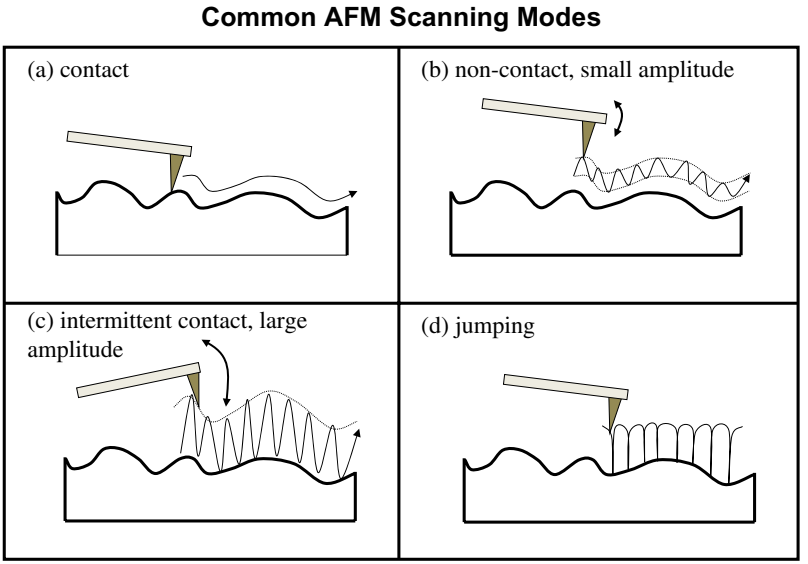


Fig. 1.6 A schematic illustrating the different scanning modes commonly employed in AFM. In (a), the contact mode of imaging where the tip is in constant contact with the substrate. In (b), the non-contact mode of imaging, where the tip oscillates sinusoidally with small amplitude while maintaining a fixed distance between tip and substrate. In (c), the intermittent contact mode where the tip "taps" the substrate during the scanning process. The amplitude of the tip oscillation is now typically larger than in (b). Note that the frequency of tip oscillation in (b) and (c) is much greater than the scanning frequency of the microscope. In (d), the "jump" mode where the tip makes physical contact with the substrate, is then lifted and moved to another location before contact with the substrate is reestablished.

## 1.5 Current Trends in Atomic Force Microscopy

The basic techniques outlined above have been extended in a number of interesting ways, producing a large family of SPMs each specially tailored to detect the local variation in some quantity of interest. This extension of SPM is sometimes referred to as dual probe microscopy because the tip not only measures topography but also some other physical parameter of interest with high lateral resolution. A few examples include an electrostatic force microscope (EFM or scanning Kelvin probe), a magnetic force microscope (MFM), a photon scanning tunnelling microscope (PSTM), a scanning electrochemical microscope (SECM), a scanning near-field optical microscope (SNOM), a scanning capacitance microscope (SCM), scanning tunnelling spectroscopy (STS), and a frictional force microscope (FFM).

Current trends seek to exploit operation of AFM under liquid, to both image and probe soft biological material. Ever faster scanning requires ever smaller cantilevers that can oscillate more rapidly, pushing the upper frequency limits of detection electronics into the MHz regime. Spatial-dependent property maps are also collected in which not only the amplitude, but also the phases of the cantilever motion relative to the cantilever driving force, are measured and interpreted. Lastly, the cantilever is no longer treated as a simple oscillating thin beam, but as a dynamic vibrating object in which higher modes of oscillation are monitored to obtain spatial dependent property maps of substrates. Higher harmonic imaging has also become popular to reconstruct the nature of the interaction force vs. cantilever tip position.

There are many books and articles that have been written to summarize these advanced developments and a listing of useful references is included at the end of this chapter.

## 1.6 Chapter Summary

The rapid evolution of SPMs since their first demonstration in the early 1980s has truly been remarkable. Largely because they are versatile and relatively inexpensive, SPMs have ushered in a world-wide interest in nanotechnology. SPMs are notable because they provide high resolution (often atomic scale) metrology. Also, it is now clear that SPM tips can be used as tools capable of nanometer manipulation and fabrication. As an example, AFM nanolithography utilizes an AFM tip to locally modify a substrate in a very precise way.

SPM operation has been extended to scanning under liquid, allowing a window into the biological world. Advances in high-speed scanning are rapidly occurring, indicating that smaller cantilevers with higher resonant frequencies may lie in the near future. Linear parallel arrays of cantilevers have been fabricated to work in a massively parallel fashion and efforts to independently control individual cantilevers in the array have also been reported. Current indicators are that technology underlying these proximal probe microscopes will continue to improve, and the scanning probe class of instruments will continue to become ever more commonplace as a tool of choice to probe the properties of nanoscale objects.

When using an AFM, no matter which mode of imaging is employed, the motion of the substrate required to keep a relevant voltage signal constant

at some pre-set value is used to form an image. In contact mode imaging, a voltage proportional to the static deflection of the cantilever is used. In non-contact mode imaging, either the amplitude or frequency of the cantilever oscillation is employed as a feedback signal.

The popularity of AFM as a core technique for surface metrology and characterization on a wide variety of different samples is now well documented. Using intermittent contact mode imaging, atomically resolved AFM images have been demonstrated that match the resolution of STM [giessibl03] [sugimoto07] [sugimoto07], but this usually requires an AFM operating under ultra-high vacuum conditions. Recent work has also demonstrated atomic resolution under water [fukuma05], [melcher13]. Under controlled conditions, the vertical resolution of AFM (typically better than 1 nm) rivals that of STM, while a force sensitivity of order 1 pN can be achieved under skilful operation.

## 1.7 Further Reading

***Chapter One References*:**

[binnig82] G. Binnig, H. Rohrer, Ch. Gerber, E. Weibel, "Tunnelling through a controllable vacuum gap", Appl. Phys. Lett., **40,** 178–80 (1982).

[binnig83a] G. Binnig, H. Rohrer, C. Gerber, E. Weibel, "7 × 7 Reconstruction of Si(111) Resolved in Real Space", Phys. Rev. Lett. **50**, 120–23 (1983).

[binnig83b] G. Binnig and H. Rohrer, "Scanning tunnelling micro-scopy", Surf. Sci. **126**, 236–244 (1983).

[binnig86] G. Binnig, C.F. Quate, C. Gerber, "Atomic Force Microscope", Phys. Rev. Lett. **56**, 930–33 (1986).

[binnig87] G. Binnig and H. Rohrer, "Scanning Tunnelling Microscopy — from Birth to Adolescence (Nobel Lecture)", Angewandte Chemie **26**, 606–614 (1987).

[fukuma05] T. Fukuma, K. Kobayashi, K. Matsushige, H. Yamada, "True atomic resolution in liquid by frequency-modulation atomic force microscopy", Appl. Phys. Lett. **87**, 034101 (2005).

[giessibl03] F.J. Giessibl, "Advances in atomic force microscopy", Rev. Mod. Phys. **75**, 949 (2003).

[gomez05] Several sections in this chapter are adapted from J. Gomez-Herrero and R. Reifenberger "Scanning Probe Microscopy" in *Encyclopedia of Condensed Matter Physics*, eds. F. Bassani, J. Leidl, P. Wyder, Elsevier Science Ltd. pgs. 172–82 (2005).

[haguenau03] F. Haguenau, P.W. Hawkes, J.L. Hutchison, B. Satiat–Jeunemaître, G.T. Simon and D.B. Williams "Key Events in the

History of Electron Microscopy", Microsc. Microanal. **9**, 96–138 (2003).

[melcher13] J. Melcher, D. Martínez-Martín, M. Jaafar, J. Gómez-Herrero and A. Raman, "High-resolution dynamic atomic force microscopy in liquids with different feedback architectures", Beilstein J. Nanotechnol. 2013, 4, 153–163.

[muller56] E. Müller and K. Bahadur, "Field Ionization of Gases at a Metal Surface and the Resolution of the Field Ion Microscope". Phys. Rev. **102**, 624 (1956).

[muller65] E.W. Müller, "Field Ion Microscopy", Science **149** (3684), 591–601 (1965).

[shmalz29] G. Shmalz Über Glätte und Ebenheit als physikalisches und physiologisches Problem, Vereines Deut. Ingen. (VDI), **73**, 1461–67 (1929).

[sugimoto07] Y. Sugimoto, P. Pou, M. Abe1, P. Jelinek, R. Pérez, S. Morita, Ó. Custance, "Chemical identification of individual surface atoms by atomic force microscopy", Nature **446**, 64 (2007).

[tipler12] P.A. Tipler and R.A. Llewellyn, *Modern Physics, $6^{th}$ edition*, (W.H. Freeman and Co., New York), 2012.

[young71] R. Young, J. Ward and F. Scire, "Observation of metal-vacuum-metal tunnelling, field emission, and the transition regime", Phys. Rev. Lett. **27**, 922 (1971).

[young72] R. Young, J. Ward and F. Scire, "The topographiner: An instrument for measuring surface microtopography", Rev. Sci. Instrum., **43**, 999 (1972).

***Further reading*:**

[baro12] *Atomic Force Microscopy in Liquid: Biological Applications*, Eds. A.M. Baro and R. Reifenberger, (Wiley-VCH, Berlin), 2012.

[bhushan] B. Bhushan and H. Fuchs, *Applied Scanning Probe Methods Vols. I–XIII* (Springer, Berlin).

[binnig99] G. Binnig and H. Rohrer, "In touch with atoms", Rev. Mod. Phys. **71**, S324–S330 (1999).

[cappella99] B. Cappella and G. Dietler, "Force distance curves by atomic force microscopy", Surf. Sci. Rep. **34**, 1–104 (1999).

[chen93] C. Julian Chen, *Introduction to Scanning Tunnelling Microscopy*, Oxford series in Optical and Imaging Sciences, Oxford University Press, New York (1993).

[garcia02] R. Garcia and R. Perez, "Dynamic atomic force microscopy methods", Surf. Sci. Rep. **47**, 197–301 (2002).

[guntherodt94] *Scanning Tunneling Microscopy I: General Principles & Applications to Clean & Adsorbate-Covered Surfaces*, Eds. H.J. Guntherodt and R. Wiesendanger, Springer-Verlag. New York (1994).

[guntherodt97] *Scanning Tunneling Microscopy II: Theory of STM & Related Scanning Probe Methods*, Eds. H.J. Guntherodt and R. Wiesendanger, Springer-Verlag, New York (1997).

[marti93] *STM and SFM in Biology*, Eds. O. Marti and M. Amrein, Academic Press, New York (1993).

[meyer04] E. Meyer, H.J. Hug, R. Bennewitz, *Scanning Probe Microscopy*, Springer, Berlin (2004).

[sarid91] D. Sarid, *Scanning Force Microscopy with applications to electric, magnetic, and atomic forces*, Oxford Series in Optical and Imaging Sciences, Oxford University Press, New York (1991).